

Development of ZnO-graphene oxide composite for enhanced photodegradation of Sandalfix orange P3R and Sandalfix Turq. blue PG dyes under irradiation of sunlight

Muhammad Saeed^{1*}, Iqra Mubarik¹, Atta-ul- Haq¹, Nadia Akram¹, Hamza Laksaci² and Muhammad Kashif Ashraf³

¹ Department of Chemistry, Government College University Faisalabad, Faisalabad, 38000, Pakistan

² Laboratoire Energie, Environnement et Système de l' Information (LEESI), Faculté des Sciences de la Matière, des Mathématiques et de l' Informatique, Université Ahmed Draia, Adrar, 01000, Algérie

³ Central Analytical Facility Division (CAFD), Pakistan Institute of Nuclear Science and Technology (PINSTECH), Nilore, Islamabad, 44000, Pakistan

* Corresponding author, E-mail: msaeed@gcuf.edu.pk

Abstract

The rapid industrial evolution has created a serious pollution problem due to the discharge of a huge amount of wastewater contaminated with organic compounds like dyes, oil, and solvents. Organic dyes contribute to a significant portion of water pollution. Traditional methods are not successful in eliminating dyes from wastewater. Sunlight-assisted photocatalysis is an attractive alternative approach for eradicating dyes from aqueous medium. Here in, the development of ZnO-decorated graphene oxide (ZnO-GO) for the photodegradation of selected dyes is reported. Sandalfix orange P3R and Sandalfix Turq. blue PG dyes were selected as model dyes to explore the catalytic performance of fabricated ZnO-GO. The Hammer and Offeman, and chemical reduction methods were followed for the synthesis of GO and ZnO-GO, respectively. The XRD, UV visible spectroscopy, surface area measurement, FTIR, and TEM were used for the characterization of ZnO-GO. More than 95% of 100 mg/L (50 mL) of each dye was degraded during 120 min of reaction duration over the ZnO-GO catalyst. ZnO-GO exhibited 2.2- and 1.9-fold catalytic activity in the degradation of Sandalfix orange P3R and Sandalfix Turq. than GO and ZnO, respectively.

Citation: Saeed M, Mubarik I, Haq A, Akram N, Laksaci H, et al. 2025. Development of ZnO-graphene oxide composite for enhanced photodegradation of Sandalfix orange P3R and Sandalfix Turq. blue PG dyes under irradiation of sunlight. *Progress in Reaction Kinetics and Mechanism* 50: e004 <https://doi.org/10.48130/prkm-0025-0004>

Introduction

Industrial progress is crucial for global economic development. However, industrial evolution has created a serious problem of pollution worldwide. Almost every industry contributes to environmental pollution. Organic pollutants like dyes and pesticides that originate from the effluents of various industries like textiles, printing, paper, cosmetics, etc. have emerged as the most serious environmental problems during the last decade^[1–4]. Water pollution is one of the four major types of pollution, alongside air pollution, noise pollution, and radiation pollution. The poor quality of water is one of the environmental and socioeconomic challenges that contribute to deteriorating human capital and poor health outcomes^[4–6]. Wastewater contaminated with these pollutants have been treated with various physical techniques (for example adsorption, osmosis, etc), and chemical techniques (for example chemical oxidation and photocatalysis). The adsorption of pollutants on various adsorbents is a common technique for the treatment of contaminated water, but it is not effective in the complete removal of the pollutants^[7,8]. Alternately, photocatalysis, which is an eco-friendly, simple, and promising technique, is a more attractive technique for the breakdown of toxic organic substances in an aqueous medium. The breakdown of toxic molecules using semiconductor materials as photocatalysts under the irradiation of sunlight is the most acceptable protocol^[9,10]. The photocatalytic breakdown of toxic organic molecules is a type of advanced oxidation process (AOP) that consists of a complete breakdown of organic molecules by oxidation with hydroxyl radicals ($\cdot\text{OH}$)^[11,12].

ZnO and TiO_2 are the two most widely studied semiconductors in photocatalysis due to their exceptional catalytic activities,

photo sensitivities, low cost, and physical, chemical, and catalytic stabilities^[13–15]. ZnO has higher catalytic properties than TiO_2 due to its unique characteristics such as wide energy difference in VB and CB (3.37 eV, the band gap), significant binding energy of exciton (60 meV), and significant mobility of electrons ($300 \text{ cm}^2 \cdot \text{V}^{-1} \cdot \text{s}^{-1}$)^[16,17]. However, high band gap energy and fast recombination of excitons suppress the visible-light-assisted catalytic applications of ZnO. Hence, the visible light cannot be harvested by ZnO. Since visible light is naturally abundant (sunlight consists of about 40% visible light), therefore a photocatalyst capable of harvesting visible light for practical applications is needed. Thus, various strategies such as the development of composites and doping of metal or non-metal atoms are adopted to enhance the photocatalytic performance of ZnO under visible light^[18–21]. The fabrication of composite material by a combination of carbon-based substances, like graphene oxide (GO), with ZnO is an effective strategy for developing visible-light-driven photocatalysts with an extended photo response and reduced exciton recombination. Graphene oxide is a thin honeycomb-like, two-dimensional carbon-based substance, in which the hybridization form of C is sp^2 . Graphene oxide is characterized by outstanding electrical and mechanical properties. Being an outstanding electron acceptor and conducting material, graphene oxide effectively transfers the electrons generated by the absorption of photons and ultimately suppresses the recombination of excitons^[22–24]. Due to its two-dimensional planar structure and greater specific surface area, graphene oxide supports various substances to become attached to it. As a result, the pollutant molecules readily adsorb on the surface of the composite photocatalyst^[25,26]. Hence, the composite formed by the hybridization of

graphene oxide with ZnO is expected to be a photocatalyst with extraordinary catalytic properties for the breakdown of toxic organic molecules due to the unique optical and electrical properties of graphene oxide. This study reports ZnO-graphene oxide (ZnO-GO) as an efficient photocatalyst for the degradation of organic dyes under natural sunlight. The Sandalfix orange P3R and Sandalfix Turq. blue PG dyes were used as model dye pollutants. Both dyes are reactive in nature. Reactive dyes are the dyes that form covalent bonds by reaction with fibers. These dyes are highly water-soluble and are commonly used for dyeing polyamide, protein, and cellulose fibers. These dyes are widely used in the textile industry. Consequently, Sandalfix orange P3R and Sandalfix Turq. blue PG were selected as representative reactive dyes for this study.

Experimentation

Chemicals

Graphite powder (Hebei Yunai New Material Technology Co., Ltd, China), sodium hydroxide (Merck, Germany), hydrogen peroxide (Scharlab, Spain), sodium nitrate (Merck, Germany), sulfuric acid, potassium permanganate, polyvinyl alcohol, and zinc acetate (Scharlau, Germany) were used as precursor materials.

Synthesis and characterization of ZnO-GO

In the first step, GO was synthesized as follows. First, 4 g graphite and 2 g sodium nitrate were added to sulfuric acid (100 mL). The suspension was kept under stirring for 30 min. Then, 14 g potassium permanganate was mixed in, and the mixture was kept under stirring for 5 h. As a result, a thick paste was formed. Then a yellowish suspension was formed by the addition of distilled water (100 mL) to a paste. The reaction was terminated by adding 40 mL of hydrogen peroxide, after which graphene oxide (GO) was collected.

In the second step, ZnO was synthesized by the precipitation method. Typically, the pH of a solution of zinc acetate was raised to 10 by dropwise addition of 0.1 M sodium hydroxide solution. The precipitate of zinc hydroxide formed was washed to remove the remaining reactants and followed by drying at 100 °C for 12 h. Then, it was calcined at 500 °C for 3 h to obtain ZnO.

In the third step, ZnO-GO was synthesized. For this purpose, 1 g as prepared GO and ZnO were suspended in 20 mL distilled water in separate beakers. Both suspensions were ultrasonicated and then mixed. Seventy mg polyvinyl alcohol was also added in mixed suspension and ultrasonicated again. The fabricated ZnO-GO was then filtered, washed, and dried.

The as-prepared ZnO-GO was characterized by advanced instrumental techniques including XRD, DR-UV-vis spectroscopy, surface area measurement, FTIR, and TEM.

Photocatalytic activity

Photocatalysis of ZnO-GO was explored by performing photodegradation of the selected dyes. A UV-visible spectrophotometer was utilized to estimate the catalytic properties of ZnO-GO. A total of 0.1g ZnO-GO was suspended in a 50 mL solution containing a known amount of either or both dyes in a beaker. The solution was then swirled for half an hour under the dark magnetically. After that, a reaction mixture sample was separated for analysis by a UV-visible spectrophotometer. Then, the suspension was irradiation with sunlight while stirring continuously. Reaction mixture samples were separated and analyzed after a time interval.

Results and discussion

Synthesis of ZnO-GO

The impregnation of ZnO nanomaterials on the surface of a GO nanosheet is due to the interactions between ZnO and hydroxyl

functional groups on GO. Furthermore, there is a delocalization of π electrons in GO resulting in a delocalized π bond. The interactions of unpaired π electrons and Zn^{2+} result in Zn-O-C linkages. Hence, ZnO-GO is formed due to the affinity of GO towards Zn^{2+} producing active sites for the attachment of ZnO on GO. All the above-mentioned factors also play a crucial role in the generation and separation of charge carriers^[27,28].

Characterization of ZnO-GO

The phase purity and crystallinity of a sample can be estimated by XRD analysis. Therefore, we performed the XRD analysis of the as-prepared ZnO-GO sample. The results of XRD analyses are given in Fig. 1. It can be observed that XRD patterns show sharp and well-resolved peaks which confirm the crystallinity of the prepared material. A peak was observed in XRD of GO at 10.4° which is a characteristic peak of GO. This peak has been indexed to the (002) plane of GO^[29,30]. Similarly, several sharp peaks can be noticed in the XRD pattern of ZnO-GO which confirms the crystalline nature of the prepared sample. These peaks include peaks at 2 theta 10.4°, 31.6°, 34.2°, 36.2°, 47.4°, 56.4°, 62.5°, and 67.9°. The peaks at 2 theta 10.4° have been indexed to the (002) plane of GO. The remaining peaks observed in XRD of ZnO-GO have been assigned to (002), (100), (101), (102), (103), (110), and (200) planes of ZnO, respectively^[31–35].

The band gap of ZnO-GO was investigated by DR-UV-visible spectroscopy. Figure 2 shows the UV-visible spectra of ZnO and ZnO-GO. It can be noticed that the formation of ZnO-GO shifts the absorption edge towards the longer wavelength side. Using Eqn (1), the band gap energy of ZnO and ZnO-GO was calculated as 3.37 and 2.91 eV, respectively. The wavelength in nm for ZnO and ZnO-GO was determined using the concept of extrapolation of the sharply rising portion and horizontal portion of the curves^[36–38]. The wavelength of intersection was determined as 368 and 426 nm for ZnO and ZnO-GO, respectively. As the band gap energy of ZnO-GO (2.91 eV) corresponds to the visible region of the radiation spectrum, therefore it can be used as a visible-light-driven photocatalyst

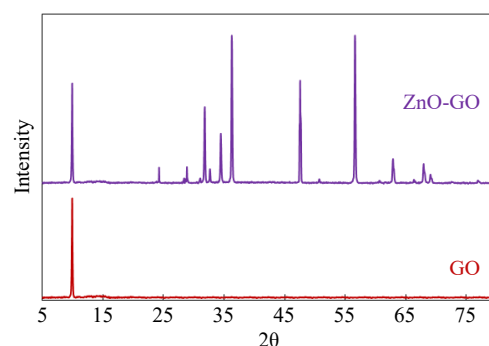


Fig. 1 XRD analysis.

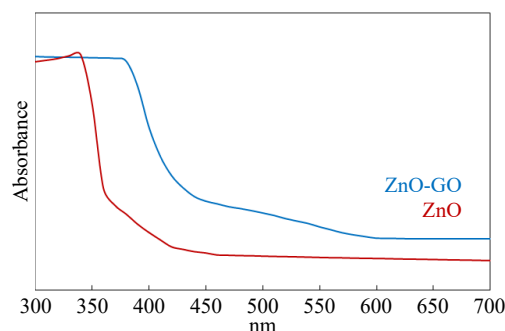


Fig. 2 DR-UV visible spectra of ZnO and ZnO-GO.

for environmental applications. The excitation of ZnO-GO by absorption of visible light is due to the dye-like photosensitizer behavior of GO in ZnO-GO^[23,39,40]. Hence, we used ZnO-GO as a photocatalyst for the photodegradation of dyes in this study.

$$\text{Bandgap Energy (eV)} = \frac{1240}{nm} \quad (1)$$

The surface area was determined by studying the adsorption-desorption of nitrogen gas on ZnO-GO. Figure 3 shows the behavior of adsorption and desorption of nitrogen on ZnO-GO. The adsorption-desorption isotherm observed as given in Fig. 3 is a type IV isotherm according to the IUPAC classification of isotherms. The hysteresis loop formed by adsorption-desorption of nitrogen is classified as H3 type. The observed type of isotherm and hysteresis loop shows the mesoporous and non-homogeneous nature of the ZnO-GO. The BET surface area was measured to be 56.5 m²·g⁻¹ for ZnO-GO, which is approximately three times greater than pure ZnO (17.4 m²·g⁻¹)^[41–43].

The functional groups associated with GO and ZnO-GO were estimated by FTIR analyses of the samples. Figure 4 depicts the results of FTIR analyses. The absorption bands at 555, 670, and 774 cm⁻¹ observed in the FTIR spectrum of ZnO-GO are representative peaks of Zn-O linkage. The bands at ~1,055 and 1,723 cm⁻¹ represent the C-O-C and C=O linkages. Similarly, the peaks at ~1,400 and ~1,600 cm⁻¹ are associated with O-H or C-OH and hydroxyl groups of H₂O, respectively^[41,44–47]. Zhou et al.^[48] have assigned the bands at 1,078 and 3,432 cm⁻¹ to the bending and stretching vibrations of the hydroxyl group.

The shape and morphology of the GO and ZnO-GO were analyzed by TEM analysis. For this purpose, the JEM 2100 JEOL transmission electron microscope was used. Figure 5 shows the obtained results. Considering the TEM of GO given in Fig. 5, it is concluded that the prepared GO is characterized by a significant level of translucency. The TEM indicates that the morphology and shape of the prepared GO is crumpled, and flat-flake-like in nature. The TEM indicates that

GO exists in the form of thin sheets. It confirms the excellent exfoliation during the fabrication of GO. Furthermore, the wrinkles and darker regions observed in TEM of GO confirm the stacking and folding of the thin sheets. The TEM of ZnO-GO (Fig. 5) reveals the homogeneous and independent distribution of ZnO on thin sheets of GO. The deposition of the ZnO particles on the sheets of GO is evident by the dark regions in the micrograph of ZnO-GO^[49–52].

Photocatalytic activity

Sandalfix orange P3R and/or Sandalfix Turq. blue PG dye were utilized as representative pollutants for the study of the catalytic activity of developed photocatalysts. Detailed information about these dyes is given in Table 1. A 50 mL solution of Sandalfix orange P3R and/or Sandalfix Turq. blue PG dye (100 mg·L⁻¹) was used as model wastewater for the study of catalytic activity. As degradation of dye due to photolysis may interfere with the photocatalytic efficiency of ZnO-GO, therefore the contribution of photocatalysis in degradation of Sandalfix orange P3R and Sandalfix Turq. blue PG dye was explored in the first step. It was accomplished by stirring the dye solution under sunlight irradiation for 2 h. The analysis of samples taken at different time intervals did not show any change in concentration solutions (Fig. 6). It confirmed that there is no degradation of Sandalfix orange P3R and Sandalfix Turq. blue PG dye due to photolysis in this study. In addition, the contribution of sorption in the removal of dye was also explored. It was carried out by stirring the dye solution containing 0.1 g ZnO-GO under dark conditions. A ~10% decrease in the concentration of Sandalfix orange P3R and Sandalfix Turq. blue PG dye was observed due to adsorption on the surface of the ZnO-GO (Fig. 6). Then, the catalytic eradication of dyes in the presence of a ZnO-GO catalyst was investigated. This investigation was accomplished by stirring the dye solution containing 0.1 g ZnO-GO under natural sunlight irradiation. The extent of photodegradation was followed by regular measurement of the absorbance of dye solution at respective wavelengths of maximum absorbance. Since the absorbance is proportional to concentration, therefore the removal of dyes was expressed as a plot of time vs C_t/C₀ as given in Fig. 6. More than 95% of each dye (100 mg·L⁻¹, 50 mL) was degraded during 120 min of reaction duration. Hence, it is confirmed that ZnO-GO can be used as an active catalyst for the sunlight-assisted photodegradation of Sandalfix orange P3R and Sandalfix Turq. blue PG dyes.

The recyclability of ZnO-GO in photodegradation of Sandalfix orange P3R and Sandalfix Turq. blue PG dyes were also investigated. The spent ZnO-GO used in photodegradation was collected and washed using ethanol and water. After drying, the spent ZnO-GO was re-used under similar experimental conditions. More than 83% of 100 mg·L⁻¹ (50 mL) of each dye was degraded during 120 min of reaction duration. Hence, the fabricated ZnO-GO is a stable and active catalyst for the photodegradation of dyes.

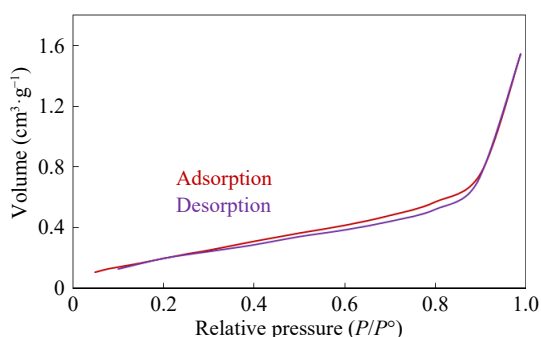


Fig. 3 Nitrogen adsorption-desorption analysis on ZnO-GO.

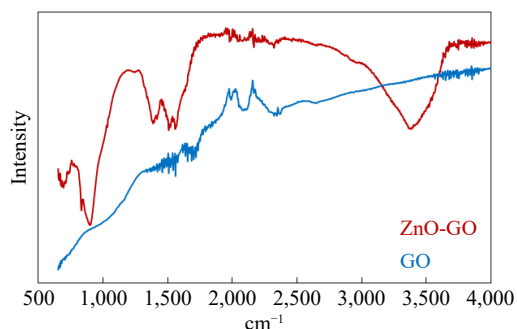


Fig. 4 FTIR analysis.

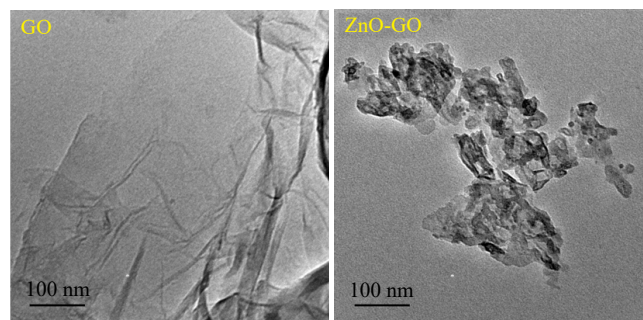
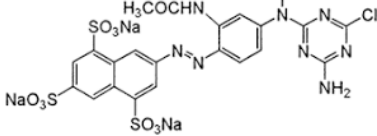
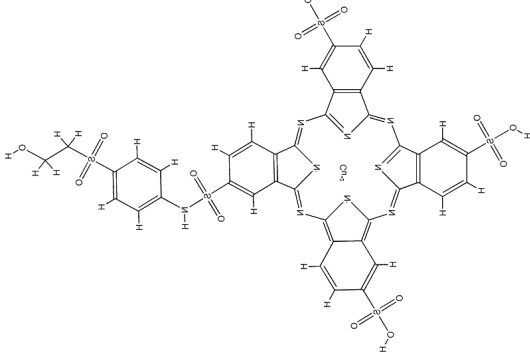
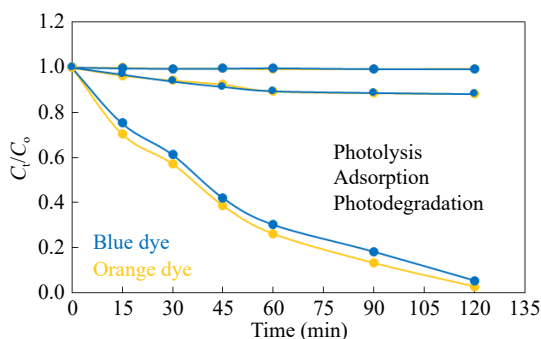
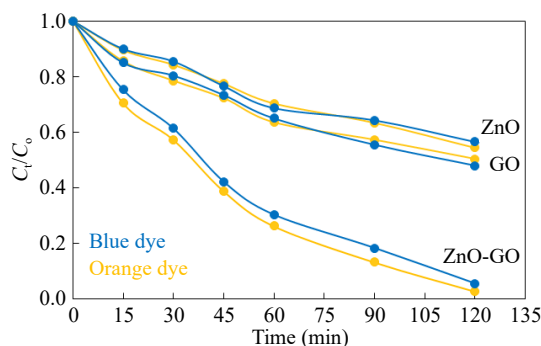


Fig. 5 TEM analysis.

Table 1. Detailed information about the selected dyes.

Name	Sandalfix orange P3R	Sandalfix Turq. blue PG
Color	Orange	Blue
Class	Reactive	Reactive
CI number	Reactive orange 12	Reactive blue 21
λ_{\max}	485 nm	414 nm
Molecular weight	793 g·mol ⁻¹	1,079.6 g·mol ⁻¹
Molecular formula	C ₂₁ H ₁₄ ClN ₈ Na ₃ O ₁₀ S ₃	C ₄₀ H ₂₅ CuN ₉ O ₁₄ S ₅
Molecular structure		

**Fig. 6** Treatment of the selected dyes with ZnO-GO. Reaction conditions: 50 mL solution having concentration 100 mg·L⁻¹ 0.1 g ZnO-GO were stirred at 40 °C.**Fig. 7** Treatment of the selected dyes with ZnO, GO, and ZnO-GO photocatalyst. Reaction conditions: 50 mL solution having concentration 100 mg·L⁻¹ 0.1 g each catalyst in separate experiments were stirred at 40 °C.

Comparison of photocatalytic activity

The effect of the formation of composite between ZnO and GO on the photodegradation of dyes was also explored. This study was conducted through photodegradation experiments using ZnO, GO, and ZnO-GO as separate components. The ZnO-GO composite showed much higher catalytic performance in the photodegradation of Sandal-fix orange P3R and Sandal-fix Turq. blue PG dyes than pristine ZnO and GO. The comparison of the catalytic performance of GO, ZnO, and ZnO-GO is given in Fig. 7. The catalytic activity of ZnO-GO was 2.2 and 1.9 folds than the activity of ZnO and GO, respectively. The higher catalytic activity of ZnO-GO is attributed to the efficient transfer of the photo-induced electrons through graphene sheets.

Mechanism and kinetics of photocatalytic degradation

Figure 8 illustrates the proposed mechanism of dye photodegradation in the presence of ZnO-GO. The catalytic efficiency of a photocatalyst depends on the contact between the photocatalyst and dye molecules, the rate of formation of electron-hole pairs, and the separation of electrons and holes. Graphene oxide (GO) has many functional groups including a π - π conjugation system. This π - π conjugation facilitates the efficient contact between dye molecules and ZnO-GO. The irradiation of dye solution containing a photocatalyst causes the excitation of ZnO-GO and dye molecules as well by

absorption of photons. The excitation of the photocatalyst creates positive holes and electrons in the valence band and conduction band of ZnO-GO, respectively. Due to electron-accepting nature of GO, the photo-induced electrons flow to the sheet of GO. As a result of the separation of electrons and positive holes, their rate of recombination is reduced. In other words, the recombination of photo-induced charges takes place through GO because its work function (−4.42 eV) is in between the VB and CB of ZnO (−7.25 and −4.05 eV, respectively). Hence, the separation of electrons due to their flow to the GO sheet causes an improvement in the catalytic performance. Similarly, the electrons of excited dye molecules also follow the GO path. Once separated, the positive holes and electrons initiate complex redox reactions and finally generate OH radicals. The OH radicals attack dye molecules and degrade them into environmentally friendly products^[53–55]. This whole process can be described in the following reactions (ZG: ZnO-GO; DY: Dye molecules).

The role played by OH radicals was verified by a scavenging experiment using benzoquinone as a scavenger for hydroxyl radicals. A 15% decrease was observed in catalytic performance in the presence of benzoquinone. It shows that OH radicals are involved in the degradation of dyes.

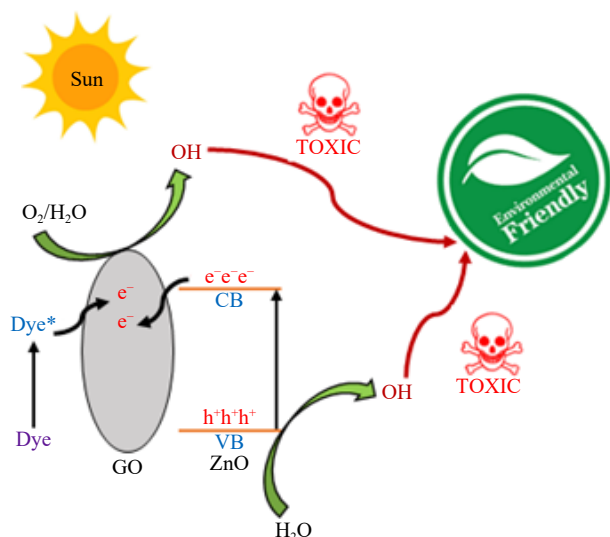
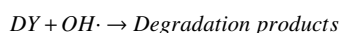
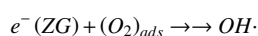
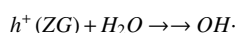
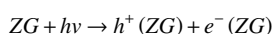


Fig. 8 Mechanism of photocatalytic degradation of dyes.



The proposed mechanism shows that the rate of reaction (r) depends on three factors: 1. Concentration of dye; 2. Adsorbed oxygen; 3. Energy of photon. Hence, we can describe the rate as:

$$r = k_r [DY] (O_2)_{ads} E_{photon} \quad (2)$$

As the reaction is taking place in an open atmosphere and under continuous irradiation, therefore the rate of reaction becomes independent of the last two factors. Hence, we can write as:

$$r = k_r [DY] \quad (3)$$

$$r = -\frac{d[DY]}{dt} = k_r [DY] \quad (4)$$

On integration and rearrangement ($[DY]_0$, $[DY]_t$ and k_r represent the initial concentration of dyes, concentration at different times, and rate constant, respectively)^[56].

$$[DY]_t = [DY]_0 e^{-k_r t} \quad (5)$$

The above rate expression was used to analyze the degradation data by the non-linear method. Figure 9 shows the fitting of the kinetics model to the experimental data. The rate constants determined are listed in Table 2 which indicate that the rate of reaction over ZnO-GO is 3.3 and 4.1 times higher than the rate of GO and ZnO, respectively.

The kinetics rate expression given in Eqns (2) and (5) shows that the rate of reaction depends on the concentration of the reactant. Therefore, the effect of the initial concentration of selected dyes on photocatalytic performance was also analyzed. For this purpose, separate photodegradation experiments in the presence of the ZnO-GO catalyst were performed using 50, 100, and 150 mg·L⁻¹ as initial concentrations of each dye. The photocatalytic performance was monitored by measurement of absorbance of the reaction mixture at different time intervals. The obtained photodegradation data was analyzed by a non-linear method of analysis according to the kinetics rate expression given in Eqn (5). The obtained results are given in Fig. 10. The rate constants determined are listed in Table 3. The kinetics expression given in Eqn (3) shows that the rate of

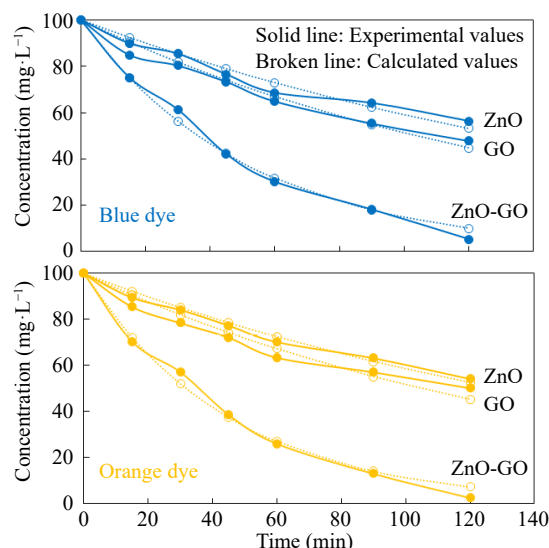


Fig. 9 Kinetics of photocatalytic degradation of the selected dyes. Reaction conditions: 50 mL (100 mg·L⁻¹) dye solution was treated with 0.1 g catalyst at 40 °C.

Table 2. Rate constants for photocatalytic degradation of the selected dyes.

Photocatalyst	Sandalfix orange P3R		Sandalfix turq. blue PG	
	k_r (per min)	R^2	k_r (per min)	R^2
ZnO	0.0054	0.99	0.0053	0.99
GO	0.0066	0.98	0.0067	0.98
ZnO-GO	0.0217	0.99	0.0191	0.99

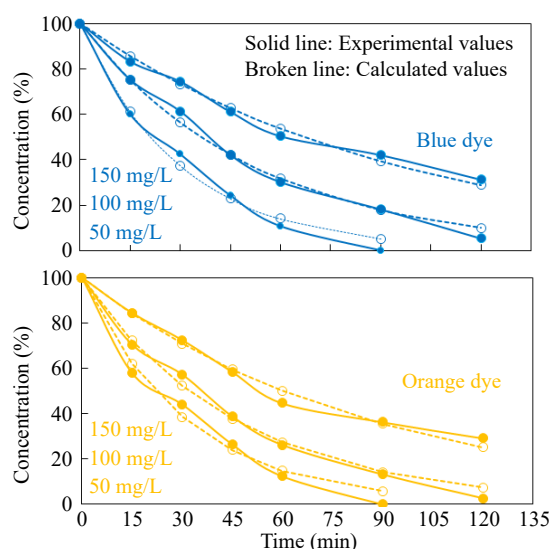


Fig. 10 Effect of concentration on catalytic activity of ZnO-GO in photodegradation of the selected dyes. Reaction conditions: 50 mL dye solution was treated with 0.1 g ZnO-GO at 40 °C.

reaction is directly proportional to the concentration of the reactant, however, the reverse trend was observed in this study. The data given in Fig. 10 and Table 3 show that the rate of photocatalytic performance decreased with an increase in concentration of Sandalfix orange P3R and Sandalfix Turq. blue PG dyes. The main reason for the decrease in photocatalytic performance is the inhibition of photons to the surface of the catalyst at higher concentrations because the photons are absorbed by dye molecules at higher concentrations. Hence higher concentration of dyes results in

Table 3. Rate constants for photocatalytic degradation of the selected dyes with different initial concentrations.

Concentration (mg·L ⁻¹)	Sandalfix orange P3R		Sandalfix Turq. blue PG	
	*Activity (%)	k _r (per min)	*Activity (%)	k _r (per min)
50	88	0.0319	89	0.0326
100	74	0.0217	70	0.0191
150	55	0.0115	50	0.0103

* Photodegradation after 60 min.

blockage of the penetration of sunlight into the surface of the catalyst^[57,58].

Conclusions

The ZnO-GO composite was successfully synthesized and characterized using various techniques, including XRD, DR-UV-vis spectroscopy, surface area measurement, FTIR, and TEM. The synthesized ZnO-GO demonstrated exceptional performance in the photodegradation of Sandalfix orange P3R and Sandalfix Turq. blue PG dyes under natural sunlight. The degradation data were analyzed using a first-order kinetic model through a non-linear approach with Solver-Excel software. The rate constants for dye photodegradation using ZnO-GO were 3.3 and 4.1 times higher than those obtained with GO and ZnO, respectively. The superior catalytic performance of ZnO-GO was attributed to the efficient transfer of photoinduced electrons facilitated by the graphene sheets. Additionally, the photocatalytic efficiency was found to be inversely proportional to the initial concentration of the dyes.

Author contributions

The authors confirm contribution to the paper as follows: conceptualization, data curation, methodology, project administration, writing - original draft; Saeed M; supervision: Saeed M, Haq A, Akram N; validation: Saeed M, Haq A; formal analysis: Mubarik I, Laksaci H; investigation: Mubarik I, Akram N; resources: Laksaci H, Ashraf MK; writing - review & editing: Saeed M, Ashraf MK. All authors reviewed the results and approved the final version of the manuscript.

Acknowledgments

The Travel Grant (Ref No. HEC/R&D/TG/212886, Date 23-08-2024) provided by the Higher Education Commission (HEC) of Pakistan for presenting this paper at the 1st International Conference on Civil and Environmental Engineering for Resilient, Smart and Sustainable Solutions organized at the College of Engineering, Prince Mohammad Bin Fahd University, AL-Khobar, Saudi Arabia during November 3-5, 2024, is acknowledged.

Conflict of interest

The authors declare that they have no conflict of interest.

Dates

Received 1 December 2024; Revised 9 January 2025; Accepted 17 January 2025; Published online 3 March 2025

References

1. Hassaan M, Nemr A El, Hassaan MA. 2017. Health and environmental impacts of dyes: mini review. *American Journal of Environmental Science and Engineering* 1:64–67

2. Luan M, Jing G, Piao Y, Liu D, Jin L. 2017. Treatment of refractory organic pollutants in industrial wastewater by wet air oxidation. *Arabian Journal of Chemistry* 10:S769–S776
3. Wang N, Zhang Z, Zhang Y, Xu X, Guan Q. 2025. Fe-Mn oxide activating persulfate for the in-situ chemical remediation of organic contaminated groundwater. *Separation and Purification Technology* 355:129566
4. Zhang Y, Xu L, Wang J, Pan H, Dou M, et al. 2024. Bagasse-based porous flower-like MoS₂/carbon composites for efficient microwave absorption. *Carbon Letters*
5. Zhang K, Ye Z, Qi M, Cai W, Saraiva JL, et al. 2025. Water quality impact on fish behavior: a review from an aquaculture perspective. *Reviews in Aquaculture* 17:12985
6. Zhang X, Usman M, Irshad AUR, Rashid M, Khattak A. 2024. Investigating spatial effects through machine learning and leveraging explainable AI for child malnutrition in Pakistan. *ISPRS International Journal of Geo-Information* 13:330
7. Li W, Mu B, Yang Y. 2019. Feasibility of industrial-scale treatment of dye wastewater via bio-adsorption technology. *Bioresource Technology* 277:157–70
8. Chaukura N, Murimba EC, Gwenzi W. 2017. Synthesis, characterisation and methyl orange adsorption capacity of ferric oxide–biochar nanocomposites derived from pulp and paper sludge. *Applied Water Science* 7:2175–86
9. Iqbal A, Haq AU, Cerrón-Calle GA, Ali Raza Naqvi S, Westerhoff P, et al. 2021. Green synthesis of flower-shaped copper oxide and nickel oxide nanoparticles via capparid decidua leaf extract for synergic adsorption-photocatalytic degradation of pesticides. *Catalysts* 11:806
10. Jabeen S, Sherazi TA, Ullah R, Ali Raza Naqvi S, Rasheed MA, et al. 2021. Electrodeposition-assisted formation of anodized TiO₂-CuO heterojunctions for solar water splitting. *Applied Nanoscience* 11:79–90
11. Al-Rawashdeh NAF, Allabadi O, Aljarrah MT. 2020. Photocatalytic activity of graphene oxide/zinc oxide nanocomposites with embedded metal nanoparticles for the degradation of organic dyes. *ACS Omega* 5:28046–55
12. Gul I, Sayed M, Rehman F, Wang J, Fu P, et al. 2024. Unlocking the potential of multifunctional and highly porous Ti₃C₂/TiO₂@Bi₂O₃ – based MXene: synergetic photocatalytic activation of peroxy monosulfate, hydrogen evolution and antimicrobial activity. *Applied Catalysis B: Environment and Energy* 359:124493
13. Siritwong C, Wetchakun N, Inceesungvorn B, Channei D, Samerjai T, et al. 2012. Doped-metal oxide nanoparticles for use as photocatalysts. *Progress in Crystal Growth and Characterization of Materials* 58:145–63
14. Kumar SG, Rao KSRK. 2014. Polymorphic phase transition among the titania crystal structures using a solution-based approach: From precursor chemistry to nucleation process. *Nanoscale* 6:11574–632
15. Zhuang Q, Li X, Lian X, Hu H, Wang N, et al. 2024. Catalysis Enhancement of Co₃O₄ through the epitaxial growth of inert ZnO in peroxy monosulfate activation: the catalytic mechanism of surface hydroxyls in singlet oxygen generation. *Crystal Growth & Design* 25:319–29
16. Wang ZL. 2004. Zinc oxide nanostructures: growth, properties and applications. *Journal of Physics Condensed Matter* 16:829–58
17. Sierra-Fernandez A, De la Rosa-García SC, Gomez-Villalba LS, Gómez-Cornelio S, Rabanal ME, et al. 2017. Synthesis, photocatalytic, and antifungal properties of MgO, ZnO and Zn/Mg oxide nanoparticles for the protection of calcareous stone heritage. *ACS Applied Materials & Interfaces* 9:24873–86
18. Zhou H, Guo J, Zhu G, Xu H, Tang X, et al. 2024. Flotation behavior and mechanism of smithsonite under the system of bidentate ligand sulfide sodium thiocyanate. *Separation and Purification Technology* 334:126086
19. Chandak VS, Kathwate LH, Kumbhar MB, Kulal PM. 2025. Spray deposited high performance Fe-doped ZnO ethanol sensor operating at low temperatures. *Journal of Industrial and Engineering Chemistry*
20. Aliaga J, Cifuentes N, González G, Sotomayor-Torres C, Benavente E. 2018. Enhancement photocatalytic activity of the heterojunction of two-dimensional hybrid semiconductors ZnO/V₂O₅. *Catalysts* 8:374
21. Wang Y, Wang J, Cai R, Zhang J, Xia S, et al. 2024. Enhanced Local CO Coverage on Cu Quantum Dots for Boosting Electrocatalytic CO₂ Reduction to Ethylene. *Advanced Functional Materials* 2024:2417764
22. Sharma M, Sondhi H, Krishna R, Srivastava SK, Rajput P, et al. 2020. Assessment of GO/ZnO nanocomposite for solar-assisted

- photocatalytic degradation of industrial dye and textile effluent. *Environmental Science and Pollution Research* 27:32076–87
23. Shalaby A, Nihitjanova D, Markov P, Staneva AD, Iordanova RS, et al. 2017. UV-assisted photocatalytic synthesis of ZnO-reduced graphene oxide nanocomposites with enhanced photocatalytic performance in degradation of methylene blue. *ECS Journal of Solid State Science and Technology* 6:M36–M43
 24. Shan Z, Yang Y, Shi H, Zhu J, Tan X, et al. 2021. Hollow dodecahedra graphene oxide-cuprous oxide nanocomposites with effective photocatalytic and bactericidal activity. *Frontiers in Chemistry* 9:755836
 25. Sabaghnia N, Janmohammadi M, Dalili M, Karimi Z, Rostamnia S. 2019. Euphorbia leaf extract-assisted sustainable synthesis of Au NPs supported on exfoliated GO for superior activity on water purification: reduction of 4-NP and MB. *Environmental Science and Pollution Research* 26:11719–29
 26. Kamran U, Rhee KY, Lee SY, Park SJ. 2022. Innovative progress in graphene derivative-based composite hybrid membranes for the removal of contaminants in wastewater: A review. *Chemosphere* 306:135590
 27. Lv X, Huang Y, Liu Z, Tian J, Wang Y, et al. 2009. Photoconductivity of bulk-film-based graphene sheets. *Small* 5:1682–87
 28. Wang J, Gao Z, Li Z, Wang B, Yan Y, et al. 2011. Green synthesis of graphene nanosheets/ZnO composites and electrochemical properties. *Journal of Solid State Chemistry* 184:1421–27
 29. Anjum F, Asiri AM, Khan MA, Khan MI, Khan SB, et al. 2021. Photo-degradation, thermodynamic and kinetic study of carcinogenic dyes via zinc oxide/graphene oxide nanocomposites. *Journal of Materials Research and Technology* 15:3171–91
 30. Shalaby A, Nihitjanova D, Markov P, et al. 2025. Structural analysis of reduced graphene oxide by transmission electron microscopy. *Bulgarian Chemical Communications* 47:291–95
 31. Karthik R, Thambidurai S. 2017. Synthesis of cobalt doped ZnO/reduced graphene oxide nanorods as active material for heavy metal ions sensor and antibacterial activity. *Journal of Alloys and Compounds* 715:254–65
 32. Tao HC, Fan LZ, Mei Y, Qu X. 2011. Self-supporting Si/Reduced Graphene Oxide nanocomposite films as anode for lithium ion batteries. *Electrochemistry Communications* 13:1332–35
 33. Ramadoss A, Kim SJ. 2013. Facile preparation and electrochemical characterization of graphene/ZnO nanocomposite for supercapacitor applications. *Materials Chemistry and Physics* 140:405–11
 34. Nuengmacha P, Chanthai S, Mahachai R, Oh WC. 2016. Visible light-driven photocatalytic degradation of rhodamine B and industrial dyes (texbrite BAC-L and texbrite NFW-L) by ZnO-graphene-TiO₂ composite. *Journal of Environmental Chemical Engineering* 4:2170–77
 35. Lonkar SP, Pillai V, Abdala A. 2019. Solvent-free synthesis of ZnO-graphene nanocomposite with superior photocatalytic activity. *Applied Surface Science* 465:1107–13
 36. Yasin M, Saeed M, Muneer M, Usman M, ul Haq A, et al. 2022. Development of Bi₂O₃-ZnO heterostructure for enhanced photodegradation of rhodamine B and reactive yellow dyes. *Surfaces and Interfaces* 30:101846
 37. Saeed M, Al-Saeed FA, Altaf M, Alahmari SD, Bokhari TH, et al. 2022. Synthesis of visible-light-driven Ag₂O-Co₃O₄ Z-scheme photocatalyst for enhanced photodegradation of reactive yellow dye. *New Journal of Chemistry* 46:23297–304
 38. Saeed M, Khan I, Adeel M, Akram N, Muneer M. 2022. Synthesis of a CoO-ZnO photocatalyst for enhanced visible-light assisted photodegradation of methylene blue. *New Journal of Chemistry* 46:2224–31
 39. Pragathiswaran C, Abbubakkar BM, Govindhan P, Abuthahir KAS. 2015. Synthesis of TiO₂ and ZnO nano composites with graphene oxide photocatalytic reduction and removal of chromium (VI) in aqueous solution. *Journal of Applicable Chemistry* 4:525–32
 40. Feng Y, Feng N, Wei Y, Zhang G. 2014. An in situ gelatin-assisted hydrothermal synthesis of ZnO-reduced graphene oxide composites with enhanced photocatalytic performance under ultraviolet and visible light. *RSC Advances* 4:7933–43
 41. Nisar A, Saeed M, Muneer M, Usman M, Khan I. 2022. Synthesis and characterization of ZnO decorated reduced graphene oxide (ZnO-rGO) and evaluation of its photocatalytic activity toward photodegradation of methylene blue. *Environmental Science and Pollution Research* 29:418–30
 42. Saeed M, Adeel S, Abdur-Raouf H, Usman M, Mansha A. 2017. ZnO catalyzed degradation of methyl orange in aqueous medium. *Chiang Mai Journal of Science* 44:1646–53
 43. Zhang GY, Feng Y, Wu QS, Xu YY, Gao DZ. 2012. Facile fabrication of flower-shaped Bi₂WO₆ superstructures and visible-light-driven photocatalytic performance. *Materials Research Bulletin* 47:1919–24
 44. Maruthupandy M, Qin P, Muneeswaran T, Rajivgandhi G, Quero F, et al. 2020. Graphene-zinc oxide nanocomposites (G-ZnO NCs): Synthesis, characterization and their photocatalytic degradation of dye molecules. *Materials Science and Engineering: B* 254:114516
 45. Azarang M, Shuhaimi A, Yousefi R, Sookhkhian M. 2014. Effects of graphene oxide concentration on optical properties of ZnO/RGO nanocomposites and their application to photocurrent generation. *Journal of Applied Physics* 116:084307
 46. Salih E, Mekawy M, Hassan RYA, El-Sherbiny IM. 2016. Synthesis, characterization and electrochemical-sensor applications of zinc oxide/graphene oxide nanocomposite. *Journal of Nanostructure in Chemistry* 6:137–44
 47. Shueb M, Singh BR, Mobin M, Afreen G, Khan W, et al. 2015. Kinetic study on mutagenic chemical degradation through three pot synthesized graphene@ZnO nanocomposite. *PLoS One* 10:0135055
 48. Zhou H, Guo J, Zhu G, Xie F, Tang X, et al. 2024. Highly efficient preparation of crystalline yttrium carbonate in sodium carbonate system: Formation and growth mechanism. *Journal of Rare Earths*
 49. Geng Y, Wang SJ, Kim JK. 2009. Preparation of graphite nanoplatelets and graphene sheets. *Journal of Colloid and Interface Science* 336:592–98
 50. Dideykin A, Aleksenskiy AE, Kirilenko D, Brunkov P, Goncharov V, et al. 2011. Monolayer graphene from graphite oxide. *Diamond and Related Materials* 20:105–8
 51. Long D, Li W, Ling L, Miyawaki J, Mochida I, et al. 2010. Preparation of nitrogen-doped graphene sheets by a combined chemical and hydrothermal reduction of graphene oxide. *Langmuir* 26:16096–102
 52. Tu TH, Cam PTN, Van Trong Huy L, Phong MT, Nam HM, et al. 2019. Synthesis and application of graphene oxide aerogel as an adsorbent for removal of dyes from water. *Materials Letters* 238:134–37
 53. Kumbhakar P, Pramanik A, Biswas S, Kole AK, Sarkar R, et al. 2018. In-situ synthesis of rGO-ZnO nanocomposite for demonstration of sunlight driven enhanced photocatalytic and self-cleaning of organic dyes and tea stains of cotton fabrics. *Journal of Hazardous Materials* 360:193–203
 54. Pirhashemi M, Habibi-Yangjeh A. 2017. Ultrasonic-assisted preparation of plasmonic ZnO/Ag/Ag₂WO₄ nanocomposites with high visible-light photocatalytic performance for degradation of organic pollutants. *Journal of Colloid and Interface Science* 491:216–29
 55. Maruthupandy M, Muneeswaran T, Vennila T, Vaishali CV, Anand M, et al. 2022. Photocatalytic efficiency of graphene/nickel oxide nanocomposites towards the degradation of anionic and cationic dye molecules under visible light. *Journal of Photochemistry and Photobiology A: Chemistry* 427:113819
 56. Saeed M, Asghar H, Khan I, Akram N, Usman M. 2025. Synthesis of TiO₂-g-C₃N₄ for efficient photocatalytic degradation of Congo Red dye. *Catalysis Today* 447:115154
 57. Balcha A, Yadav OP, Dey T. 2016. Photocatalytic degradation of methylene blue dye by zinc oxide nanoparticles obtained from precipitation and sol-gel methods. *Environmental Science and Pollution Research* 23:25485–93
 58. Saeed M, Alwadai N, Ben Farhat L, Baig A, Nabgan W, et al. 2022. Co₃O₄-Bi₂O₃ heterojunction: an effective photocatalyst for photodegradation of rhodamine B dye. *Arabian Journal of Chemistry* 15:103732



Copyright: © 2025 by the author(s). Published by Maximum Academic Press, Fayetteville, GA. This article is an open access article distributed under Creative Commons Attribution License (CC BY 4.0), visit <https://creativecommons.org/licenses/by/4.0/>.